USING U-NETS FOR ACCURATE R-PEAK DETECTION IN FETAL ECG RECORDINGS

Peishan Zhou and Stephen So and Belinda Schwerin

School of Engineering, Griffith University, Gold Coast, Australia

ABSTRACT

Electrocardiography (ECG) is a promising approach for continuous fetal heart rate monitoring. Its morphology can provide information on fetal health to guide patient care by clinicians. However, fetal ECGs extracted from abdominal ECGs are often too weak to reliably detect fetal heart rate. This study evaluates the application of a U-Net architecture for accurate R-peak detection in low-SNR fetal ECG signals. The proposed method achieves high accuracy with a positive predictive value of 99.81%, sensitivity of 100.00%, and an F1-score of 99.91% on direct fetal ECG from the Abdominal and Direct ECG Database, with significantly reduced false predictions, and outperforming two other baseline methods compared with. Notably, our approach demonstrates robustness, accurately predicting peaks in regions of high distortion, a capability unmatched by other methods evaluated. This finding indicates the suitability and benefits of the U-Net architecture for peak detection in fetal ECG signals.

KEYWORDS

U-Net, R-Peak Detection, QRS Detection, Fetal ECG

1. INTRODUCTION

Fetal heart rate (FHR) and fetal heart rate variability (FHRV) are important indicators of potential complications or changes in fetal wellbeing [1], and thereby used to direct interventions and subsequent care. Typically, Cardiotocography (CTG) is used for non-invasive Fetal heart rate monitoring (FHRM), however this can only be used in short intervals, includes averaging over multiple beats reducing accuracy, and is not suitable for longer term monitoring. More recently, electrocardiography (ECG) has been shown to be a promising alternative technology to achieve continuous FHRM [2], with the potential to enable clinicians to monitor fetal wellbeing with improved context. It also offers the advantage of providing fetal ECG (FECG) morphology information, enabling identification of potential abnormalities [3]. Thus, reliable processing of FECG signals, particularly R-peak detection associated with fetal heart rate (FHR) acquisition, is important for improving outcomes in prenatal care.

FECG can be obtained non-invasively from electrodes placed on the mother's abdomen, or directly on the scalp of the fetus. While scalp electrode FECG has higher SNR, it can only be done at delivery and therefore is not suitable for continuous FHRM. Non-invasive FECG (NI-FECG), on the other hand, while suitable for continuous FHRM, faces a number of challenges. Firstly, abdominal ECG (AECG) includes a mix of FECG, maternal ECG (MECG), and other artifacts associated with fetal movements, respiration, and interference from other power equipment [4]. The FECG signal is weak relative to the MECG, and therefore overwhelmed by the MECG signal. Therefore, the MECG needs to be removed from the abdominal signal first. Further, since the FECG and MECG as well as other physiological source interferences are mixed

David C. Wyld et al. (Eds): SIPRO, EMSA, CCSEA- 2024
pp. 01-11, 2024. CS & IT - CSCP 2024 DOI: 10.5121/csit.2024.140901

in both the time and frequency domains [5], the low signal-to-noise ratio (SNR) of the extracted FECG signal often leads to inaccurate or even failure of R-peak detection. In addition, since the characteristics of the fetal ECG signal is different from that of adults, existing R-peak detection methods for adult ECG signals have reduced performance for fetal ECG. FHR is almost double the adult HR, and the fetal QRS-complex amplitude is strongly dependent on lead, gestational age, and fetus position [6].

The importance and challenges associated with reliable extraction of accurate R-peak locations from AECG has inspired a considerable body of work in the area. Works generally focus on either removal of the MECG in order to improve the quality of the FECG signal, or improving R-peak detection from the resulting FECG signal, with the former of these attracting the most attention. Various algorithms have been proposed for MECG suppression, such as template subtraction [7]-[9], adaptive filtering [10], [11], blind source separation (BSS) [12], [13], or deep-learning based algorithms [14]-[16]. For extensive reviews of different approaches, see [12] or [17]. Other works, including this one, have focused on improving the accuracy and reliability of R-peak detection from the resulting FECG signal.

For detection of R-peaks in FECG, variations of the Pan-Tompkins method are popularly used. The Pan-Tompkins algorithm (PTA) is a well-known QRS complex wave detection algorithm proposed in 1985 [18] for adult ECG. Adaptations of PTA for fetal R-peak detection have been used with some success [19-21]. For example, Agostinelli et all. [22] adapted the original PTA to better account for fetal ECG characteristics, with parameters modified to account for differences in heart rate, QRS-complex amplitudes and QRS duration compared to adult ECGs. They also included an R-peak corrector algorithm, resulting in improved detection reliability. However, PTA-based approaches still face inherent challenges, including the inability to suppress noise resulting in poor performance for low SNR signals [23], and being prone to false R-peak detections.

U-Net is a deep convolutional neural network (CNN) architecture initially designed for 2D image segmentation tasks, employing an encoder-decoder structure. Its structure includes contracting paths to capture context and symmetric expanding paths for precise positioning, enabling it to represent the relationships between different image components. Moreover, incorporating skip connections helps it to mitigate overfitting, making it effective in scenarios with limited training data. It has been proven successful with minimal data training across various applications, achieving end-to-end image segmentation [24].

More recently, the U-Net structure has been applied to 1D tasks, including predicting blood pressure [25], speech enhancement [26], and adult heartbeat detection [27]. In a study by Mai et al. [28], a deep learning model combining U-NET and Bidirectional Long Short-Term Memory for automatic heartbeat detection based on ballistocardiogram signals demonstrated the superior performance and robustness of the U-NET model across three signal-to-noise ratio (SNR) ranges, highlighting its resilience to signal noise and interference including respiratory and motion artifacts. Zahid et al. [29], in a comparative evaluation of two open-access electrocardiogram databases, found that the U-NET structure outperformed five other algorithms. The observed robustness of U-NET resulted in a significant reduction in the false positive rate of Holter ECG signals by more than 54% and a significant reduction in the false negative rate by 82%.

Motivated by these findings, this work evaluates the suitability of U-NET architecture for the detection of R-peaks in low-SNR FECG signals where false positive detections are a significant problem by traditional methods. The architecture of the proposed fetal R-peak detection method is adapted from the traditional 2D U-NET model to fit the 1D time-series task. The robustness of the proposed algorithm is verified on the direct FECG signal (the gold standard) contained in the

Abdominal and Direct Fetal Electrocardiogram Database (A&D FECGDB). Two PTA-based methods are also simulated for horizontal comparison with our proposed method to verify the robustness of our algorithm. The remainder of this paper is organised as follows. Section II describes the proposed peak detection method. Section III describes the details of experiments conducted and metrics used. Section IV presents and discusses results from experiments, and Section V draws conclusions and future directions.

2. METHODOLOGY

Figure 1 provides an overview of each stage of the proposed fetal R-peak detection method.

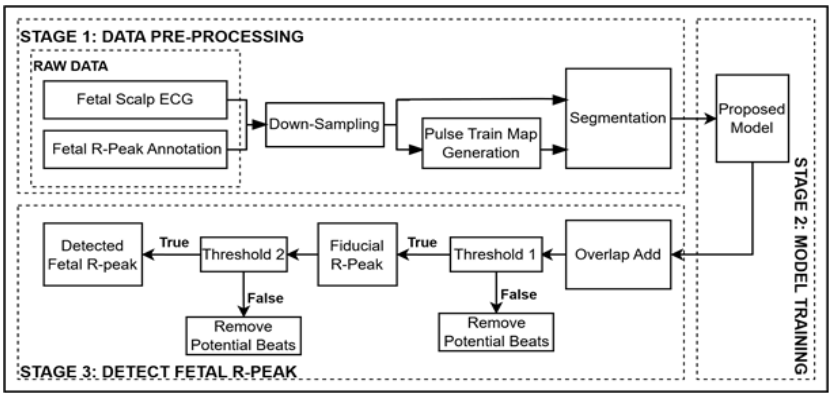

Figure 1. Flow diagram for the proposed U-NET fetal R-Peak detection method.

2.1. Data Pre-Processing

This first stage describes processing and preparation which is to applied to both training and testing data. First, the 1 kHz fetal ECG signal is downsampled to 250 Hz. Opting for high sampling rates involves a balance between capturing more signal detail and allocating additional storage space and computational resources [30]. In contrast, lower sampling rates are sufficient for most clinical applications and are more practical in terms of data storage and processing requirements. Moreover, the sampling rate of commonly used public fetal electrocardiogram databases is 250 Hz. Hence, to mitigate heightened computational costs without substantial benefits, this study downsampled the signal to 250 Hz. Additionally, this approach offers greater flexibility for adapting the model to various test datasets.

Inspired by the ideas presented in [29], the peak detection task was formulated as a 1D segmentation problem that had achieved great success in adult R-peak detection. A pulse train map was generated based on the true peak annotations, with each pulse sharing the same width and being centred on the R-peak position. The pulse representation involves labelling each pulse as a series of ones, while zeros signify other sampling points. This methodology not only highlights the peak area but also aids in achieving data balance, thereby addressing potential challenges associated with imbalanced labels. In this study, a pulse width of 15 samples was chosen. This decision aligns with findings from Chivers et al. [31], wherein an algorithm for measuring cardiac time intervals in fetal ECG indicated an average range for fetal QRS-complex duration of between 54.72ms (manual measurement) and 58.34ms (algorithm measurement). This range corresponds to 13.68-14.50 sample points under a 250 Hz sampling frequency condition. Moreover, upon inspecting the morphology of the A&D database, it was observed that the QRS-complex typically spans 15 sample points. Figure 2 illustrates an example of raw fetal scalp ECG signal along with the corresponding generated pulse sequence map.

The next step is segmentation, where a fixed sliding window of 1000 samples (equivalent to four seconds) was used. Furthermore, the shifting update for the sliding window was configured to 200 samples. The processed segments of ECG data and corresponding pulse train maps were saved in a two-dimensional matrix to be used in subsequent U-NET model training.

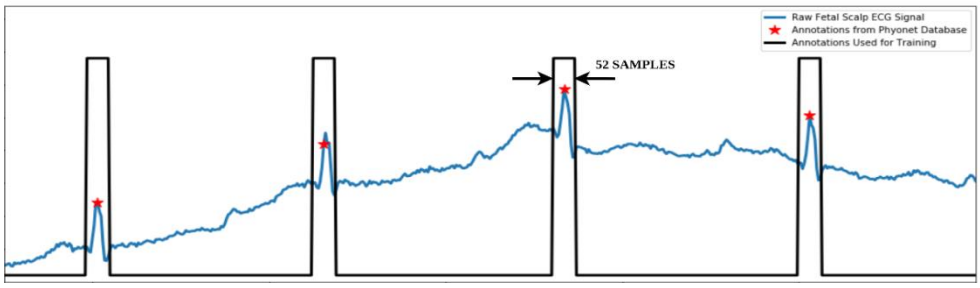

Figure 2. An example of the raw fetal scalp ECG (direct FECG) signal and corresponding pulse train map generated. The red star represents the true R-peak annotation specified in the dataset. Each 52 sample wide pulse is centred about this true annotation to form the pulse train used for training.

2.2. Training Stage

In the second stage, the model undergoes training using the constructed inputs and pulse train map data for training signals. The architecture of the proposed U-NET neural network is illustrated in Figure 3. The scalp ECG segments are first sent to the U-NET through the encoding stage, and the output of the 1D-convolutional (1D-CNN) layer is saved before going through the max pooling layer. This is followed by decoding blocks to achieve the up-sampling process via 1D deconvolution (transpose) convolutional layer. The output of the 1D transpose CNN layer is skip connected with the output of the 1D-CNN layer pre-stored in the encoding stage. Finally, the output of the last activation function is fed to the last convolution layer to obtain a predicted pulse train map with a Sigmoid activation function.

Both the encoder blocks and decoder blocks are composed of three 1D-CNN layers. The bottleneck block consists of two 1D-CNN layers. The filter parameters and kernel size in the convolutional layer in the encoding block were {16, 16, 32} and {9,9,6} respectively. Each convolutional layer is followed by a ReLU activation function. A max-pooling layer with a pool size of 2 is connected after each 1D-CNN layer to achieve dimensionality reduction. In the decoding block, the filter parameters and kernel sizes were {32, 16, 16} and {9, 9, 6} for the 1D-CNN layer and 1D deconvolutional CNN layer, respectively. The stride of the deconvolution layer is set to 2.

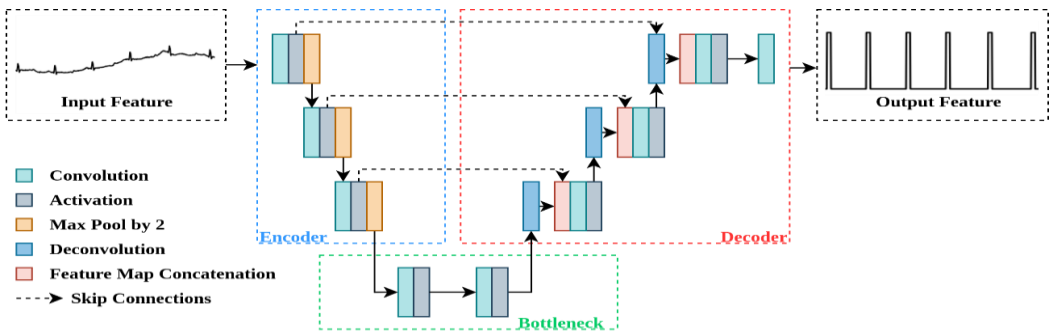

Figure 3. Proposed U-NET Architecture for R-peak detection from Fetal Electrocardiogram.

The parameters of the model were randomly initialised during training. Binary cross entropy was selected as the loss function used by the model. The Adam optimiser was used to minimise the Loss between the predicted and the original pulse train map. Five-fold cross-validation was performed using four records as the training set and the remaining record as the test set. The learning rate was set to 0.001, with a batch size of 64. Each model was trained for 400 epochs.

2.3. Fetal R-peak Detection

In the testing, R-peak detection stage, constructed inputs from test signals are applied to the model constructed in the training stage. The model's output feature is a pulse train representing predictions of potential R-peak locations, which undergoes additional post-processing steps to identify and eliminate false positives, thereby enhancing the accuracy of R-peak detection.

The output map segments are restored to a full length through an overlap-add process, and additional processing steps are executed to finalise the peak screening process. Firstly, a filtering criteria removes potential false positive predictions where amplitudes of the output pulse train are weak and below the first threshold (*Thres_small*). Currently, the threshold *Thres_small* is set to a fixed value of 0.3 to eliminate these weak false positive predictions. This means that predicted values below *Thres_small* will be converted to 0 and the remaining values will be converted to 1. Next, the middle value of each pulse is taken to generate a fiducial R-peak series, corresponding to predicted R-peak locations. Finally, a second threshold (*Thres_close*) is applied to eliminate closely spaced potential beats. Since the fetal heart rate variability is in the range of 110-160 bpm [3], *Thres_close* of 81 sampling points is used to filter potential R peaks that are too close to be physically possible. Where two beats are closer than this threshold, the beat further from midpoint of preceding and subsequent beats is removed. The result is a pulse train where the centre of each pulse corresponds to the location of a predicted R-peak within the original FECG signal.

2.4. A&D Database

This work employed the Abdominal Direct Fetal Electrocardiogram Database (A&D FECGDB) due to its inclusion of direct fetal ECG. The database contains five records from five different subjects, numbered r01, r04, r07, r08 and r10. Each recording lasts for five minutes and is sampled at 1 kHz with 16-bit resolution. The annotation of the fetal R-wave position provided within the database had been automatically determined for the direct FECG signal by online analysis in the KOMPOREL system, and then the precise R-wave position was manually verified by a team of cardiologists [32], [33].

3. EXPERIMENTS

To evaluate the performance of the proposed R-peak detection method, a comparison of performance to PTA-based methods commonly used in the literature was done. Below we provide details of these methods, and how metrics used to evaluate performance were applied.

3.1. Methods Included for Comparison

This work compares the performance of the proposed U-Net method for detecting fetal R-peaks with the Pan-Tompkins Algorithm (PTA), which is commonly used for comparison in the literature. Details of the general algorithm for PTA are shown in flow chart Figure 4 Here, we include a comparison with two PTA-based implementations, namely Mathworks (denoted PTA_M) and ECGPUWAVE (denoted PTA_E). The choice of the open-source PTA-based

implementations was based on its suitability for the R-peak detection task. PTA_Mathworks is an implementation of PTA provided by Mathworks, and details can be found in [34]. ECGPUWAVE is part of Physionet Tool Kit [33] and details can be found at: https://physionet.org/content/ecgpuwave/1.3.4/ . While ECGPUWAVE is based on PTA, it also includes improvements utilising slope information.

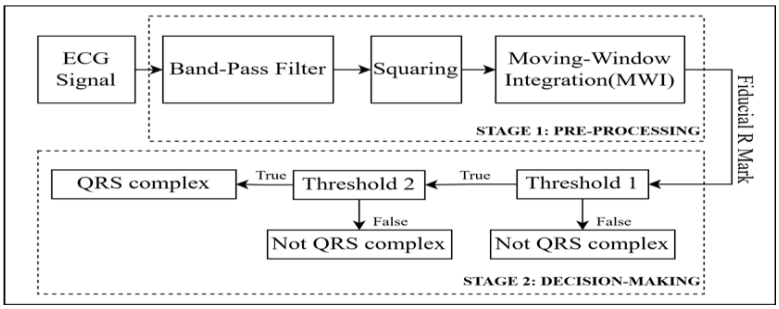

Figure 4. Multiple processing steps of Pan-Tompkins algorithm. In brief, the PTA algorithm detects the R-peak after two stages: the preprocessing stage to achieve R-wave enhancement; and the decision-making stage to locate R-peaks.

3.2. Evaluation Metrics

In accordance with the ANSI/AAMI guideline [35], sensitivity (SEN), positive predictability value (PPV) and F1-score allow for the assessment of the presence of R-peaks within a tolerance window. Each of these metrics have been used to evaluate the performance of the proposed method.

PPV is a measure of accuracy, which shows the ability of the algorithm to detect real annotations in all the tests performed. SEN is a measure of completeness, which shows the model's ability to find true annotations. F1-score is the harmonic average of PPV and SEN. In this study a match window size of 52 milliseconds (13 samples) is applied to determined the true positives (TP), true negatives (TN), false positives (FP). Their calculation equations are shown in Equation (1), (2) and (3), respectively.

$$PPV = \frac{TP}{TP+FP} \times 100\% \quad (1)$$

$$SEN = \frac{TP}{(TP+FN)} \times 100\% \quad (2)$$

$$F1 = \frac{2 \times PPV \times SEN}{(PPV+SEN)} \times 100\% \quad (3)$$

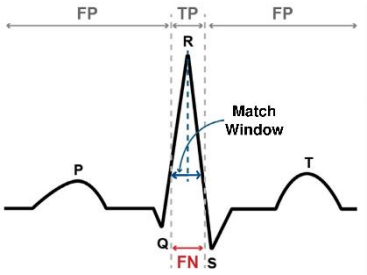

Figure 5. Important annotations of the ECG waveform. Where the predicted peak is within the match window, it is considered a TP, while predictions outside this range are considered as FP. FN indicates that the algorithm did not predict a peak within the match window of the true peak.

4. RESULTS AND DISCUSSION

The experiments compared the performance between the proposed method and two PTA-based baseline methods is undertaken. The performance of each method are shown in the following tables. Table 1 provides an overview of the average performance across all tested records for each method. From Table 1, results show that across all approaches, the proposed method consistently attains the most elevated scores across the three evaluation metrics, with average scores on PPV, SEN and F1-score of 99.81%, 100.00% and 99.91%, respectively. PTA_ECGPUWAVE performed relatively poorly in each test. Its highest F1-score[84.93%] did not exceed 85%, which is significantly lower than the scores of PTA_Mathworks [97.95%] and UNET [99.91%]. Table 2 provides more specific details on the performance of each method on individual test records, including TP, FP, FN numbers, as well as PPV, SEN, and F1-score. Notably, the proposed method achieves perfect scores of 100% for SEN, PPV and F1-score on records r01, r04, r07, and r08. FP and FN scores are considerably improved for UNET compared to both PTA_E and PTA_M methods.

Table 1. The average results in terms of PPV, SEN and F1-SCORE for each method. Entries in bold indicate highest value for that metric.

METHOD	PPV (%)	SEN (%)	F1-SCORE (%)
PTA_E [33]	82.87	82.33	83.41
PTA_M [34]	97.95	97.86	98.04
UNET	**100.00**	**99.84**	**99.92**

Table 2. Performance of three methods across each test record. The method with the highest score in each test record is marked in bold.

TEST RECORD	METHOD	TP	FP	FN	PPV (%)	SEN (%)	F1-SCORE (%)
r01	PTA_E [33]	623	26	21	95.99	96.74	96.37
	PTA_M [34]	641	4	3	99.38	99.53	99.46
	UNET	**644**	**0**	**0**	**100.00**	**100.00**	**100.00**
r04	PTA_E [33]	513	141	119	78.44	81.17	79.78
	PTA_M [34]	613	27	19	95.78	96.99	96.38
	UNET	**632**	**0**	**0**	**100.00**	**100.00**	**100.00**
r07	PTA_E [33]	380	257	247	59.65	60.61	60.13
	PTA_M [34]	609	18	18	97.13	97.13	97.13
	UNET	**627**	**0**	**0**	**100.00**	**100.00**	**100.00**
r08	PTA_E [33]	636	14	15	97.85	97.7	97.77
	PTA_M [34]	645	4	6	99.38	99.08	99.23
	UNET	**651**	**0**	**0**	**100.00**	**100.00**	**100.00**
r10	PTA_E [33]	515	131	122	79.72	80.85	80.28
	PTA_M [34]	621	15	16	97.64	97.49	97.56
	UNET	**632**	**0**	**5**	**100.00**	**99.22**	**99.61**

The presence of five FN predictions by UNET in r10 caught our attention and was associated predominately with several unusually large regions where there was little evident signal or annotated beats in the FECG signal, potentially due to signal loss or poor contact of the electrode. Example segments from this record are shown, along with predictions by each method, in Figure 6, with an example of the unusual morphology of the signal where a FN was observed shown in Figure 6(b). Both PTA_E and PTA_M misjudge small noise variations in the rising trend of the signal as a R-peaks, resulting in falsely labelled beats (FP) for this region, while UNET did not.

In Figure 7(a), the improved resistance to noise of UNET is shown, with PTA_E falsely predicting a nearby noise spike and missing a beat. Figure 7. shows a segment containing a sudden large spike within the signal. Both PTA algorithms made incorrect predictions while UNET was not affected. The PTA_E method incorrectly identifies the spike as R-peak due to its large amplitude, and ignores the correct R-peak on the left. The PTA_M method was also affected by the abnormal shape and made a false positive prediction. Overall, UNET demonstrates a robust ability to detect fetal heartbeats, even in the presence of abnormal morphology.

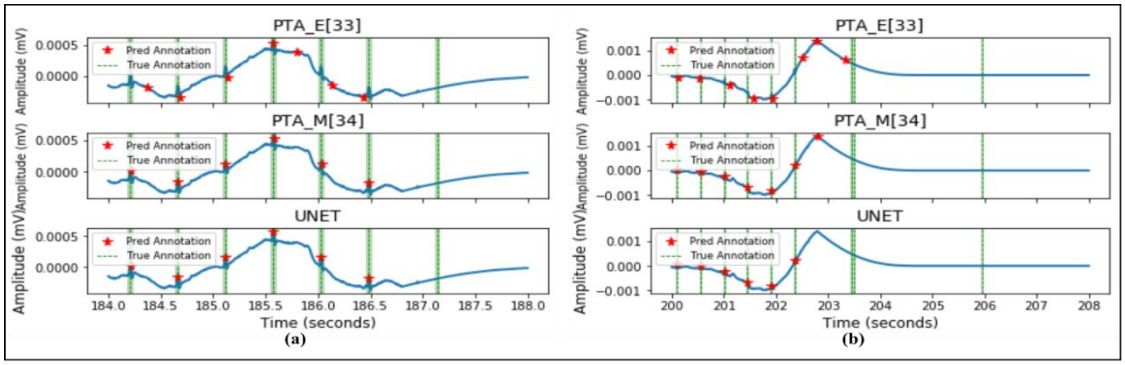

Figure 6. Example of 2 segments with unusual morphology in record r10, which features extended areas without beats. Predicted beats in this region are shown by red stars for each method, while green bands indicate annotated true beat locations.

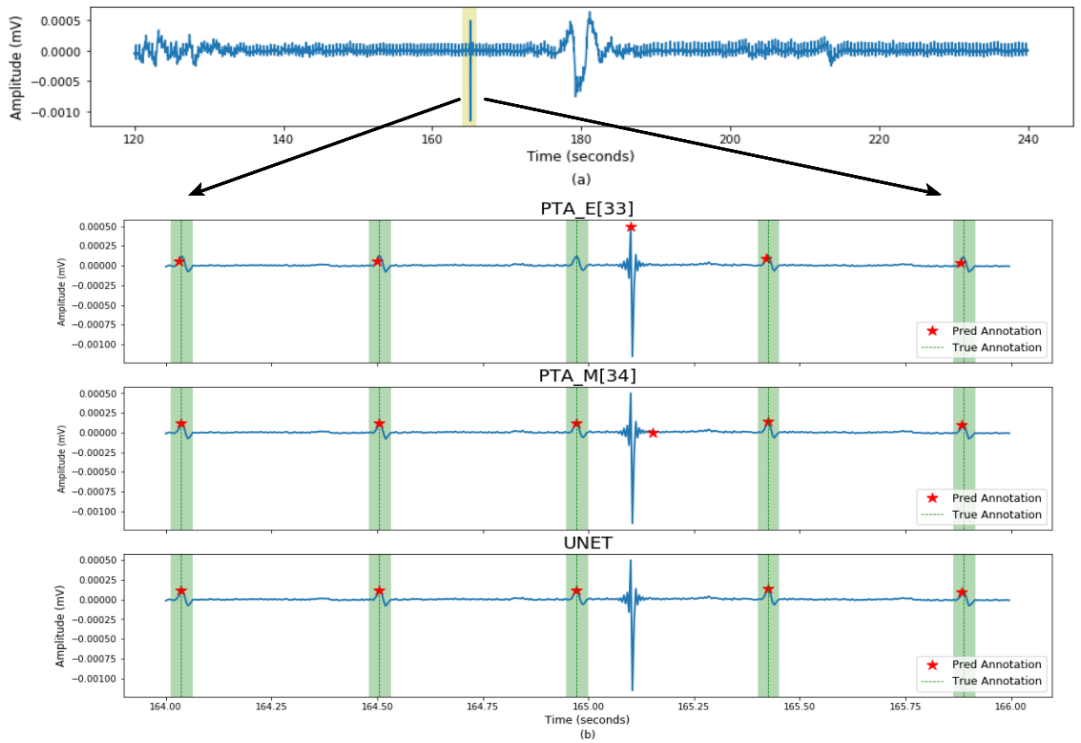

Figure 7. (a) The morphology of a 120-second segment of record r08 in A&D FECG database. Regions of unusual morphology, specifically spikes with significant amplitude, are highlighted in yellow. (b) Zoomed-in visualization of the region in record r08 containing unusual spike, alongside predictions from each of the testing methods in this region. Predicted R-peaks are indicated by red stars. 52ms tolerance range (match window) is indicated by green highlight.

5. CONCLUSIONS

In conclusion, the current work describes a novel application of the UNET architecture to enable detection of R-peaks in fetal ECG signals. The proposed method showcases high performance metrics, achieving a PPV of 99.81%, SEN of 100.00%, and an F1-score of 99.91%. In contrast, PTA_ECGPUWAVE and PTA_MATHWORKS, with respective PPVs of 84.15% and 97.86%, SENs of 85.72% and 98.04%, and F1-scores of 84.93% and 97.95%, fall short of the proposed method's performance. Notably, our method exhibits significant robustness by avoiding FP and FN in most records, unlike other two methods, which have a higher incidence of both types of errors. Furthermore, our method shows remarkable adaptability by correctly predicting abnormal morphology, a capability that cannot be replicated by the other two methods, which experienced varying degrees of failure in this regard. Overall, our proposed U-Net based method is highly accurate, confirming its potential as a powerful solution for R-peak detection in fetal ECG signals. Future work will explore its generalizability and performance on fetal ECG extracted from abdominal ECG and subjected to different types and levels of noise distortions.

REFERENCES

[1] N. Dia, J. Fontecave-Jallon, M. Resendiz, M.-C. Faisant, V. Equy, D. Riethmuller, P.-Y. Gumery, B. Rivet, (2022) "Fetal heart rate estimation by non-invasive single abdominal electrocardiography in real clinical conditions," Biomedical Signal Processing and Control, vol. 71, article 103187.

[2] G. D. Clifford, I. Silva, J. Behar, G. B. Moody, (2014) "Non-invasive fetal ECG analysis," Physiological Measurement, vol. 35, no. 8, pp. 1521–1536.

[3] R. Sameni, G. D. Clifford, (2010) "A review of fetal ECG signal processing; issues and promising directions," The open pacing, electrophysiology & therapy journal, vol. 3, pp. 4–20.

[4] M. S. Vadivu, G. Kavithaa, (2023) "Fetal qrs complexes detection using deep learning technique," Journal of Electrical Engineering & Technology, pp. 1–10.

[5] M. A. Hasan, M. B. I. Reaz, M. I. Ibrahimy, M. S. Hussain, J. Uddin, Detection and processing techniques of fecg signal for fetal monitoring, Biological procedures online 11 (1) (2009) 263–295.

[6] A. Agostinelli et al., (2015) "Noninvasive fetal electrocardiography: an overview of the signal electrophysiological meaning, recording procedures, and processing techniques," Annals of Noninvasive Electrocardiology, vol. 20, no. 4, pp. 303–313.

[7] S. Cerutti, G. Baselli, S. Civardi, E. Ferrazzi, A. Marconi, M. Pagani, G. Pardi, (1986) "Variability analysis of fetal heart rate signals as obtained from abdominal electrocardiographic recordings," Journal of perinatal medicine, vol. 14, no. 6, pp. 445–452.

[8] S. M. M. Martens, C. Rabotti, M. Mischi, R. J. Sluijter, (2007) "A robust fetal ECG detection method for abdominal recordings," Physiological measurement, vol. 28, no. 4, pp. 373–388.

[9] R. Vullings, C. H. L. Peters, R. J. Sluijter, M. Mischi, S. G. Oei, J. W. M. Bergmans, (2009) "Dynamic segmentation and linear prediction for maternal ECG removal in antenatal abdominal recordings," Physiological measurement, vol. 30, no. 3, pp. 291–307.

[10] R. Vullings, B. de Vries, J. W. M. Bergmans, (2011) "An adaptive Kalman filter for ECG signal enhancement," IEEE Transactions on Biomedical Engineering, vol. 58, no. 4, pp. 1094–1103.

[11]]F. Andreotti et al., (2014) "Robust fetal ECG extraction and detection from abdominal leads," Physiological measurement, vol. 35, no. 8, pp. 1551.

[12] S. Ravindrakumar, K. B. Raja, (2010) "Fetal ECG extraction and enhancement in prenatal monitoring — review and implementation issues," in: Trendz in Information Sciences Computing(TISC2010), pp. 16–20.

[13] L. de Lathauwer, B. de Moor, J. Vandewalle, "Fetal electrocardiogram extraction by blind source subspace separation, (2000) "IEEE Transactions on Biomedical Engineering, vol. 47, no. 5, pp. 567–572.

[14] W. Zhong, L. Liao, X. Guo, G. Wang, (2019) "Fetal electrocardiography extraction with residual convolutional encoder–decoder networks," Australasian Physical Engineering Sciences in Medicine, vol. 42, no. 4, pp. 1081–1089.

[15] A. Rasti-Meymandi, A. Ghaffari, (2021) "AECG-DecompNet: abdominal ECG signal decomposition through deep-learning model," Physiological Measurement, vol. 42, no. 4, article 045002.

[16] M. R. Mohebbian et al., (2022) "Fetal ECG extraction from maternal ECG using attention-based CycleGAN," IEEE Journal of Biomedical and Health Informatics, vol. 26, no. 2, pp. 515–526.
[17] R. Sameni, G. D. Clifford, (2010) "A review of fetal ECG signal processing; issues and promising directions," The open pacing, electrophysiology & therapy journal, vol. 3, pp. 4–20.
[18] J. Pan, W. J. Tompkins, (1985) "A real-time QRS detection algorithm," IEEE transactions on biomedical engineering, vol. 3, pp. 230–236.
[19] A. Matonia, J. Jezewski, K. Horoba et al., (2006) "The maternal ECG suppression algorithm for efficient extraction of the fetal ECG from abdominal signal," in: 2006 International Conference of the IEEE Engineering in Medicine and Biology Society, IEEE, pp. 3106–3109.
[20] S. Mirza, K. Bhole, P. Singh, (2020) "Fetal ECG extraction and QRS detection using independent component analysis," in: 2020 16th IEEE International Colloquium on Signal Processing Its Applications (CSPA), pp. 157–161.
[21] S. Sarafan et al., (2020) "Investigation of methods to extract fetal electrocardiogram from the mother's abdominal signal in practical scenarios," Technologies, vol. 8, no. 2.
[22] A. Agostinelli et al., (2017) "Noninvasive fetal electrocardiography part I: Pan-Tompkins' algorithm adaptation to fetal R-peak identification," The open biomedical engineering journal, vol. 11, no. 1, pp. 17–24.
[23] M. Fariha, R. Ikeura, S. Hayakawa, S. Tsutsumi, (2020) "Analysis of Pan-Tompkins algorithm performance with noisy ECG signals," in: Journal of Physics: Conference Series, vol. 1532, IOP Publishing, p. 012022.
[24] O. Ronneberger, P. Fischer, T. Brox, (2015) "U-net: Convolutional networks for biomedical image segmentation," in: Medical and Computer-Assisted Intervention–MICCAI 2015: 18th International Conference, Munich, Germany, October 5-9, 2015, Proceedings, Part III, Springer, pp. 234–241.
[25] S. Mahmud et al., (2022) "A Shallow U-Net architecture for reliably predicting blood pressure (BP) from photoplethysmogram (PPG) and electrocardiogram (ECG) signals," Sensors, vol. 22, no. 3.
[26] H.-S. Choi et al., (2019) "Phase-aware speech enhancement with deep complex U-Net," arXiv preprint arXiv:1903.03107.
[27] S. Vijayarangan, V. R., B. Murugesan, P. S.P., J. Joseph, M. Sivaprakasam, (2020) "RPNet: A deep learning approach for robust R-peak detection in noisy ECG," in: 2020 42nd Annual International Conference of the IEEE Engineering in Medicine Biology Society (EMBC), pp. 345–348. doi:10.1109/EMBC44109.2020.9176084.
[28] Y. Mai et al., (2022) "Non-contact heartbeat detection based on ballistocardiogram using U-Net and bidirectional long short-term memory," IEEE Journal of Biomedical and Health Informatics, vol. 26, no. 8, pp. 3720–3730.
[29] M. U. Zahid et al.,(2022) "Robust R-peak detection in low-quality Holter ECGs using 1D convolutional neural network," IEEE Transactions on Biomedical Engineering, vol. 69, no. 1, pp. 119–128.
[30] M. Mohebian, S. Vedaei, K. Wahid, A. Dinh, H. Marateb, K. Tavakolian, (2021) "Fetal ECG extraction from maternal ECG using attention-based CycleGAN," IEEE Journal of Biomedical and Health Informatics.
[31] S. Chivers et al., (2022) "Measurement of the cardiac time intervals of the fetal ECG utilising a computerised algorithm: A retrospective observational study," JRSM Cardiovascular Disease, vol. 11.
[32] J. Jezewski et al., (2012) "Determination of the fetal heart rate from abdominal signals: evaluation of beat-to-beat accuracy in relation to the direct fetal electrocardiogram," Biomedical Engineering, vol. 57, no. 5, pp. 383–394.
[33] A. L. Goldberger et al., (2000) "Physiobank, physiotoolkit, and physionet: components of a new research resource for complex physiologic signals," Circulation, vol. 101, no. 23, pp. 215–220.
[34] H. Sedghamiz, (2014) "Matlab implementation of pan tompkins ecg qrs detector," Code Available at the File Exchange Site of MathWorks.
[35] N. Association for the Advancement of Medical Instrumentation et al., (1998) "Testing and reporting performance results of cardiac rhythm and st segment measurement algorithms," ANSI/AAMI EC38 1998, p. 46.

AUTHORS

Peishan Zhou received her BEng degree with Honors in Electrical and Electronics Engineering at Griffith University, Australia in 2019. Currently she is a PhD candidate at Griffith University. Australia. Her research interests include digital signal processing and machine learning for applications of speech, and biomedical signals and images.

Stephen So received his BEng degree with First Class Honours in Microelectronic Engineering at Griffith University, Australia in 1999 and his PhD in image and speech signal processing in 2005. Currently he is a Senior Lecturer in the School of Engineering and Built Environment, Griffith University, Australia. Dr. So is a Senior Member of the IEEE and was a former member of the Editorial Board of Digital Signal Processing (published by Elsevier). His research interests are in digital signal processing of images, speech, biomedical signals as well as machine learning and deep neural networks.

Belinda Schwerin received her BEng degree with First Class Honours in Microelectronic Engineering at Griffith University, Australia in 2008, and her PhD in speech signal processing in 2013. She also has a Bachelor of Science majoring in Mathematics and IPT, and a Post Graduate Diploma in Education. Currently she is a Senior Lecturer in the School of Engineering and Built Environment, Griffith University, Australia. Her research interests include digital signal processing and machine learning for applications of speech, and biomedical signals and images.